Chemical Science

ROYAL SOCIETY OF CHEMISTRY

EDGE ARTICLE

View Article Online
View Journal | View Issue

Cite this: *Chem. Sci.*, 2021, **12**, 13037

All publication charges for this article have been paid for by the Royal Society of Chemistry

Received 5th August 2021
Accepted 3rd September 2021

DOI: 10.1039/d1sc04296c

rsc.li/chemical-science

Substituted aromatic pentaphosphole ligands – a journey across the p-block†

Christoph Riesinger, Gábor Balázs, Michael Seidl and Manfred Scheer *

The functionalization of pentaphosphaferrocene [Cp*Fe(η^5-P_5)] (**1**) with cationic group 13–17 electrophiles is shown to be a general synthetic strategy towards P–E bond formation of unprecedented diversity. The products of these reactions are dinuclear [{Cp*Fe}$_2${$\mu,\eta^{5:5}$-$(P_5)_2EX_2$}][TEF] (EX_2 = BBr_2 (**2**), GaI_2 (**3**), [TEF]$^-$ = [Al{OC(CF_3)$_3$}$_4$]$^-$) or mononuclear [Cp*Fe(η^5-P_5E)][X] (E = CH_2Ph (**4**), $CHPh_2$ (**5**), $SiHPh_2$ (**6**), $AsCy_2$ (**7**), SePh (**9**), TeMes (**10**), Cl (**11**), Br (**12**), I (**13**)) complexes of hetero-bis-pentaphosphole ((*cyclo*-P_5)$_2$R) or hetero-pentaphosphole ligands (*cyclo*-P_5R), the aromatic all-phosphorus analogs of prototypical cyclopentadienes. Further, modifying the steric and electronic properties of the electrophile has a drastic impact on its reactivity and leads to the formation of [Cp*Fe($\mu,\eta^{5:2}$-P_5)SbICp‴][TEF] (**8**) which possesses a triple-decker-like structure. X-ray crystallographic characterization reveals the slightly twisted conformation of the *cyclo*-P_5R ligands in these compounds and multinuclear NMR spectroscopy confirms their integrity in solution. DFT calculations shed light on the bonding situation of these compounds and confirm the aromatic character of the pentaphosphole ligands on a journey across the p-block.

Introduction

Electrophilic aromatic substitution is one of the most basic and widely applied reactions for the functionalization of aromatic organic compounds. While Friedel–Crafts alkylation and acylation are in fact textbook examples for the reactivity of benzene derivatives,[1] they can also be applied to smaller ring systems.[2] In contrast, derivatives of the carbocyclic aromatic cyclopentadienide anion (Cp^-, $C_5H_5^-$) form non-aromatic cyclopentadiene derivatives (CpR, C_5H_5R) upon salt metathesis with element halogenides. Compared to their alkali metal salts, transition metal (TM) bound Cp^- ligands (*e.g.* in Cp_2Fe)[3] exhibit a different reactivity towards electrophiles mimicking that of benzene derivatives (*e.g.* $(C_6H_6)Cr(CO)_3$).[4] The isolobal relationship between the CH fragment and the P atom[5] and the diagonal relationship between carbon and phosphorus suggest a comparable reactivity for the pentaphospholide anion *cyclo*-P_5^-.[6] However, investigations on the reactivity of the salts of *cyclo*-P_5^- towards alkylhalogenides showed further aggregation to polyphosphides,[7] leaving the chemistry of pentaphospholes *cyclo*-P_5R to theoretical studies for decades.[8] Similar to Cp^-, *cyclo*-P_5^- can be stabilized within the coordination sphere of different TMs[9] and is thus closely associated with the TM-mediated conversion of P_4.[10] One of the most prominent examples of such complexes is pentaphosphaferrocene [Cp*Fe(η^5-P_5)] (**1**).[9a] While **1** readily reacts with various monovalent metal salts to form coordination compounds,[11] we could also demonstrate both its redox reactivity[12] and its behavior towards anionic[13] and neutral nucleophiles.[14] These reactions yielded complexes with bent *cyclo*-P_5R ligands (**I**, Scheme 1),[13,14] which are also accessible by the reaction of a niobium

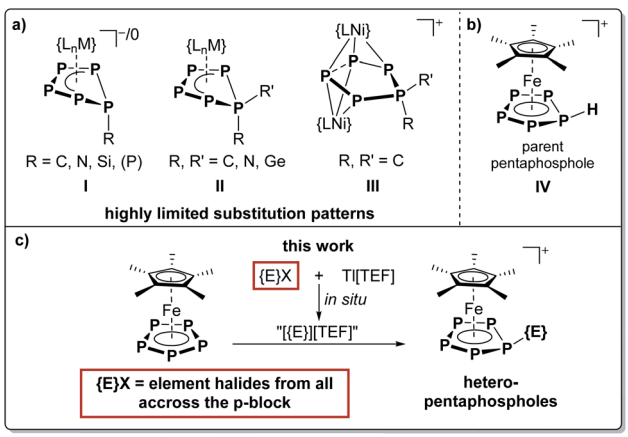

Scheme 1 (a) Known substituted *cyclo*-P_5 ligand architectures **I** ({L_nM} = {(Mes^{neo}PentN)$_2$Nb} or {Cp*Fe}), **II** ({L_nM} = {Cp*Fe}, {Cp^{PEt}Co}$^+$, {(BIAN)Co}), **III** (L = Cp^{PEt}); (b) the parent pentaphosphole complex **IV**; (c) targeted functionalization of an iron bound pentaphospholide ion with *in situ* generated cationic electrophiles from across the p-block to yield unprecedented coordinatively stabilized hetero-pentaphospholes.

Institute of Inorganic Chemistry, University of Regensburg, 93040 Regensburg, Germany. E-mail: manfred.scheer@chemie.uni-regensburg.de

† Electronic supplementary information (ESI) available. CCDC 2083554–2083563 and 2101248. For ESI and crystallographic data in CIF or other electronic format see DOI: 10.1039/d1sc04296c

phosphorus triple bond complex with P_4.[15] Disubstituted *cyclo*-P_5R_2 moieties (**II** and **III**, Scheme 1) could be obtained *via* the coordination of the respective $[P_5R_2]^+$ cations[16] to low-valent transition metal fragments.[17] The formation of the structural motif **II** was also observed upon condensation of an anionic *cyclo*-P_4 complex with chlorophosphines.[18] The introduction of germylene substituents has recently been achieved by the reaction of **1** with a digermylene.[19] While their structural motifs are remarkable, the respective *cyclo*-P_5R_n ligands (n = 1, 2) within types **I–III** do not show any aromatic character, since they do not represent pentaphospholes (**IV**).[8] Only recently, we succeeded in the synthesis of the first transition metal complexes $[Cp^*Fe(\eta^5\text{-}P_5R)][B(C_6F_5)_4]$ (**IV**, R = H, Me, $SiEt_3$) featuring such pentaphosphole ligands.[20] While our previous approach is well-suited to prepare the parent compound with a *cyclo*-P_5H ligand, it is limited to group 14 electrophiles (such as CH_3/$SiEt_3$) as introducible substituents.[21]

Thus, we sought a more general strategy to electrophilically functionalize **1** which may also be applicable beyond the synthesis of the targeted hetero-pentaphosphole complexes to other heteroaromatic ligands. Such a strategy would represent a valuable contribution to electrophilic substitution reactions in general. We hypothesized that the *in situ* generation of cationic electrophiles from p-block element halogenides and a suitable halide-abstracting reagent, as has for example been utilized for the functionalization of coordinated chlorophosphines,[22] and subsequent reaction with **1** could provide this reactivity. Such an approach would allow P–E bond formation with a nearly unlimited choice of electrophiles and would thus overcome the limitations of known synthetic strategies towards the P–E bond formation in the vicinity of transition metals.[14,15,23] Indeed, the major drawback of the so far used strategies is their immensely limited applicability to a very narrow range of electrophile/nucleophile combinations. This is usually reflected in the use of rather exotic low-valent main group species such as tetrylenes,[14b,18] $\{Cp^*Al\}_4$,[24] or the utilization of highly reactive, *e.g.* anionic, polyphosphorus ligand complexes.[23e,f] While our goal is the functionalization of **1** to obtain unprecedented hetero-pentaphosphole ligands, namely the aromatic all-P congeners of cyclopentadienes, we expect our approach to also be applicable to polyphosphorus ligand complexes of various sizes. Furthermore, this idea merges the functionalization of TM polyphosphorus complexes with the concept of electrophilic substitution,[2] a classic organic or organometallic (for *e.g.* Cp_2Fe (ref. 3) or $(C_6H_6)Cr(CO)_3$ (ref. 4)) reaction. Thus, it may be transferred back to these fields and allow the electrophilic functionalization of still challenging substrates such as multi-functionalized CpR derivatives.[25] To achieve the *in situ* generation of the desired electrophiles from the respective halogenides, Tl[TEF] ($[TEF]^- = [Al\{OC(CF_3)_3\}_4]^-$)[26] was chosen to facilitate efficient halide abstraction and simultaneously introduce the weakly coordinating $[TEF]^-$ anion. However, for some cases, we also provide an easily accessible alternative avoiding Tl^+ salts by the reaction of simple element hydrides with $[Ph_3C][B(C_6F_5)_4]$ for *in situ* electrophile generation. This method has been employed *e.g.* for the generation of the highly reactive silylium ion precursor $[(Et_3Si)_2(\mu\text{-}H)][B(C_6F_5)_4]$.[21] However, the question arises as to how broad, if successful, the applicability of this approach would actually be, and which electrophiles could be introduced by employing it. We herein report on a synthetic strategy allowing the functionalization and P–E bond formation of **1** with twelve distinct cationic electrophiles all across the p-block elements and compare their structural and electronic properties.

Results and discussion

Starting with group 13 electrophiles, we investigated the reactivity of **1** towards BBr_3 in the presence of Tl[TEF]. However, performing the reaction in a 1 : 1 : 1 stoichiometry leads to a reaction of the *in situ* prepared borinium cation $[BBr_2]^+$ with the solvent, resulting in a mixture of products (see ESI†). Repeating the reaction in the presence of a second equivalent of **1** afforded the bimetallic compound $[\{Cp^*Fe\}_2\{\mu,\eta^{5:5}\text{-}(P_5)_2BBr_2\}][TEF]$ (**2**), featuring an unprecedented$\{(cyclo\text{-}P_5)_2BBr_2\}$ ligand (Scheme 2). After workup, **2** could be isolated in 70% yield. To our pleasure, exchanging BBr_3 for the heavier analog GaI_3 affords the isostructural compound $[\{Cp^*Fe\}_2\{\mu,\eta^{5:5}\text{-}(P_5)_2GaI_2\}][TEF]$ (**3**) in 32% yield. While we had already been able to demonstrate the silylation and methylation of **1**,[20] we now wanted to broaden the scope of group 14 functionalized pentaphosphole derivatives, by using better accessible and easier-to-handle electrophile precursors. In both cases, the reaction of **1** with $PhCH_2Br$ and Ph_2CHCl in the presence of Tl[TEF] affords the pentaphosphole complexes $[Cp^*Fe(\eta^5\text{-}P_5CH_2Ph)][TEF]$ (**4**) and $[Cp^*Fe(\eta^5\text{-}P_5CHPh_2)][TEF]$ (**5**) in a yield of 45% and 80%, respectively. To demonstrate an easily accessible alternative pathway towards the electrophile generation avoiding the use of Tl^+ salts, we chose to react **1** with Ph_2SiH_2 in the presence of one equivalent of $[Ph_3C][B(C_6F_5)_4]$. A rapid reaction is indicated by the color change of the solution from green to greenish red and, after simple workup, the product $[Cp^*Fe(\eta^5\text{-}P_5SiHPh_2)][B(C_6F_5)_4]$ (**6**) could be isolated in an astonishing 85% yield. In principle, it should be possible to prepare phosphino-pentaphosphole complexes similarly well as they benefit from the additional stabilization caused by P–P bond formation. However, attempts to prepare such phosphino-functionalized species are seriously affected by the inherently high tendency of halogenophosphines to form phosphinophosphonium ions under Lewis acidic conditions.[27] We were able to observe the desired cation $[Cp^*Fe(\eta^5\text{-}P_5PBr_2)]^+$ spectroscopically only after reacting **1** with PBr_3 and Tl[TEF] at −80 °C (see ESI†). This cation, however, undergoes rapid fragmentation and rearrangement processes above −60 °C, affording a complex mixture of several polyphosphorus compounds and thus prohibiting its isolation even at low temperatures. In contrast, the reaction of **1**, Cy_2AsBr and Tl[TEF] proceeds smoothly, and from the filtered solution, the arsino-pentaphosphole complex $[Cp^*Fe(\eta^5\text{-}P_5AsCy_2)][TEF]$ (**7**) could be isolated in 68% yield. When both the electronic and steric properties of the pnictogenium cation were changed and **1** was reacted with $Cp'''SbI_2$ ($Cp''' = 1,2,4\text{-}{}^tBu_3C_5H_2$) and Tl[TEF], the unique triple-decker-like complex $[Cp^*Fe(\mu,\eta^{5:2}\text{-}P_5)SbICp'''][TEF]$ (**8**) with a P_5 middle deck could be obtained in 24% yield. The molecular

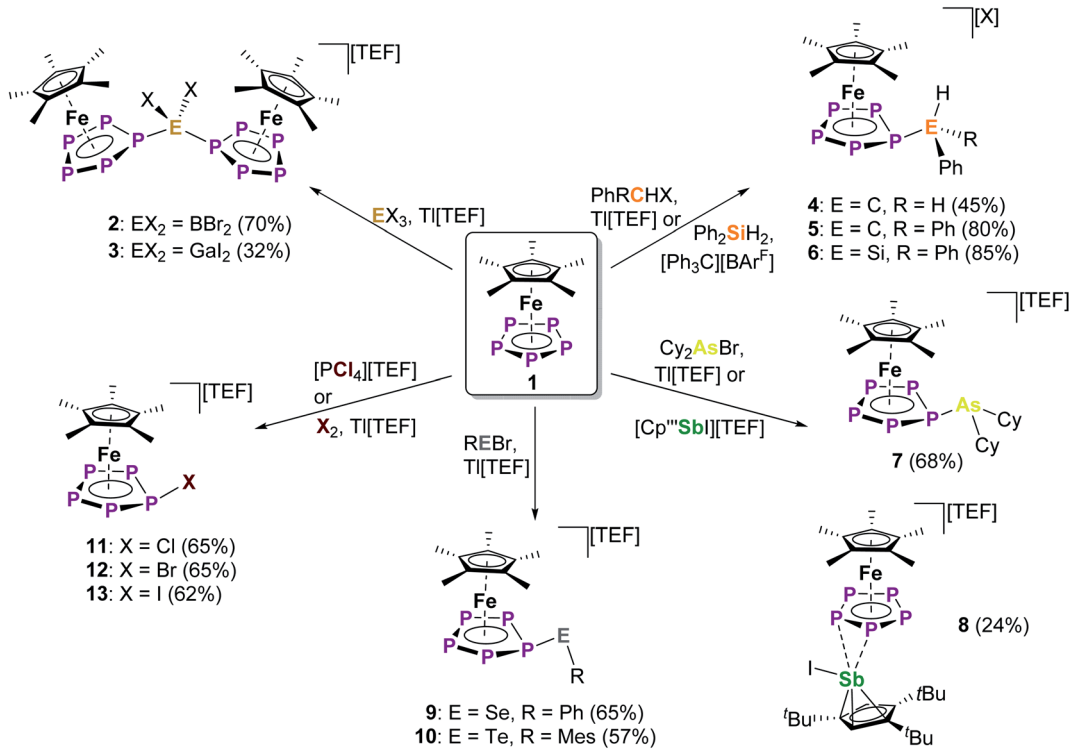

Scheme 2 Reactivity of pentaphosphaferrocene **1** with different cationic p-block electrophiles; reactions were carried out in *o*-DFB and stirred at room temperature for several hours (for details see ESI†); while all other compounds are obtained as their $[TEF]^-$ salt, **6** has a $[B(C_6F_5)_4]^-$ counterion; $[TEF]^- = [Al\{OC(CF_3)_3\}_4]^-$; while all displayed reactions are quantitative (by NMR), the yields provided are those for the crystalline compounds.

structure of **8** may provide insight into the mechanism of the electrophilic functionalization of **1** which initially seems to occur through the π-system and not by the lone pairs of one of the P atoms of the *cyclo*-P_5 ligand. Functionalization of **1** with group 16 electrophiles could be achieved by the reaction with Tl[TEF] and PhSeBr or MesTeBr, respectively. The products $[Cp^*Fe(\eta^5\text{-}P_5ER)][TEF]$ (**9**: E = Se, R = Ph; **10**: E = Te, R = Mes) could be isolated in 65% and 57% yield, respectively, and reveal novel seleno- or telluro-pentaphosphole ligands. To date, there is no synthetic pathway for a rational and selective monohalogenation of unsubstituted polyphosphorus frameworks, although the products would provide both insight into the mechanism of P_n halogenation reactions[28] and a high potential for further functionalization. After recently investigating the complex iodination chemistry of **1** (ref. 29) and of the diphosphorus complex $[\{CpMo(CO)_2\}_2(\mu,\eta^{2:2}\text{-}P_2)]$,[30] we were wondering if electrophilic halogen transfer could lead to the desired reactivity. Indeed, when a solution of $[PCl_4][TEF]$ is added to **1** in *o*-DFB, the NMR spectra of the crude solution indicate the clean conversion to $[Cp^*Fe(\eta^5\text{-}P_5Cl)][TEF]$ (**11**) and PCl_3. After workup, **11** can be isolated in 65% yield. Similarly, the addition of X_2 to mixtures of **1** and Tl[TEF] leads to the formation of $[Cp^*Fe(\eta^5\text{-}P_5X)][TEF]$ (**12**: X = Br; **13**: X = I), which could be isolated in 65% and 62% yield, respectively. Notably, these halogenation reactions can be scaled up to at least 2 mmol, allowing the gram scale preparation of **11–13**, which opens broad perspectives for their further functionalization. While the starting material **1** is comparably robust, the pentaphosphole complexes **2–13** are highly sensitive towards both moisture and air, while retaining decent thermal stability. All compounds **2–13** can be crystallized from mixtures of *o*-DFB or CH_2Cl_2 and *n*-hexane either at room temperature or at −30 °C. However, incommensurate modulation (**11**) or extreme disorder of anion and cation (**12**) within **11** and **12** prohibit a satisfactory refinement of their crystal structure. Compound **8** reveals a triple-decker-like arrangement (Fig. 1) of the cation $[Cp^*Fe(\mu,\eta^{5:2}\text{-}P_5)SbICp'''][^+]$ with elongated P–Sb interactions (3.236(2)/3.400(2) Å) and a planar P_5 ligand. The cations in **4–7** and **9–13** show the anticipated pentaphosphole complex structure with a slightly bent *cyclo*-P_5R ligand (Fig. 1). In contrast, the cations in **2** and **3** are dinuclear complexes in which two {Cp*Fe} units are bridged by the respective $\{(cyclo\text{-}P_5)_2EX_2\}$ (**2**: E = B, X = Br, **3**: E = Ga, X = I) ligand. The P–P bond lengths within **2–13** are similar and in between the sum of the covalent radii of P–P single and double bonds.[31] As observed for the parent compound $[Cp^*Fe(\eta^5\text{-}P_5H)]^+$,[20] the substituents in the hetero-pentaphosphole complexes **2–7** and **9–13** are oriented in exo-fashion regarding the envelope of the P_5 ring (Fig. 1). The respective P–E bond lengths (**2**: 1.985(7) Å, **4**: 1.853(4) Å, **5**: 1.866(4) Å, **7**: 2.348(1) Å, **9**: 2.2234(7) Å, **10**: 2.438(2) Å, **13**: 2.385(1) Å) are in the range of single bonds, whereas those in **3** (2.410(1)/2.387(1) Å) and **6** (2.3053(8) Å) are elongated compared to the sum of the respective covalent radii (P–Ga: 2.35 Å, P–Si: 2.27 Å).[31] The slight folding of the P_5 ring in these pentaphosphole complexes is far

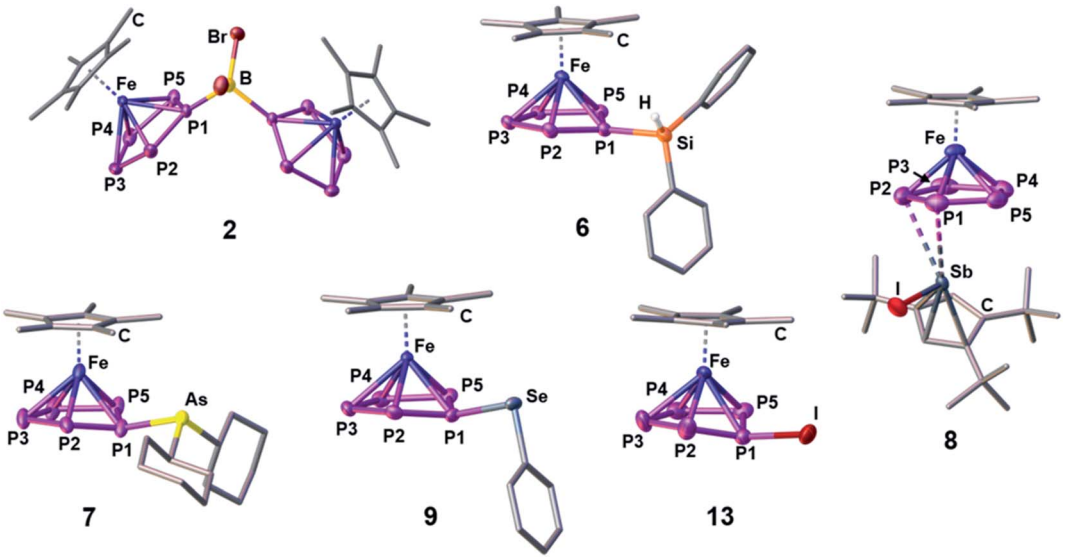

Fig. 1 Molecular structures of the cations in **2**, **6**, **7**, **8**, **9** and **13** in the solid state; Structural models for the cations in **3**, **4**, **5**, **10** and **12** as well as a list of selected structural parameters (bond lengths and angles) for all compounds can be found in the ESI.†

less pronounced than in anionic or neutral substituted *cyclo*-P_5R ligands possessing an envelope structure (type I, Scheme 1).[13,14] Interestingly, this slight folding, represented by the pyramidalization at the P_1 atom (359.94°(2) – 350.41°(13)), gradually increases when going from group 13 to group 17 substituents at the pentaphosphole ligand. To elaborate the molecular structure of the obtained pentaphosphole complexes **2–13** in CD_2Cl_2 solution, they were investigated by multinuclear NMR spectroscopy. In general, all of them reveal the expected signals for the Cp* ligand and the respective substituents in the ^{1}H NMR spectra. Furthermore, the signals for the benzylic hydrogen atoms in **4** ($\delta = 4.42$ ppm) and **5** ($\delta = 5.93$ ppm) show a coupling to the P_5 moiety (**4**: $^2J_{H-P} = 11.2$ Hz, $^3J_{H-P} = 3.2$ Hz, **5**: $^2J_{H-P} = 17.3$ Hz). Interestingly, the isostructural **6** does not show a similar coupling for the hydrogen atom bound to silicon, which we attribute to the dynamic behavior of this compound in solution. Accordingly, the $^{13}C\{^1H\}$ NMR spectra of **4** and **5** both reveal signals for the benzylic carbon atoms, which show $^1J_{C-P}$ coupling of 23 Hz for both compounds. The $^{31}P\{^1H\}$ NMR spectra of most of the obtained products reveal complex AMM′XX′ (**4**, **5**), AA′BB′X (**7**), AA′MXX′ (**11**), AA′MM′X (**6**, **9**, **12**) or even $AA'M_2M'_2X_2X'_2$ (**2**) spin systems (see ESI†). However, **3**, **8**, **10** and **13** show a highly dynamic behavior in CD_2Cl_2 solution which cannot be resolved, not even at −80 °C. Similar dynamic broadening of signals has been observed for the parent compound[20] and might be caused by a tumbling process of the respective substituent around the P_5 ring. When comparing the $^{31}P\{^1H\}$ NMR spectra (Fig. 2), the signal assigned to P_1 (according to Fig. 1) gradually shifts to higher fields going from group 13 to group 17 substituents at the pentaphosphole moiety. Similarly, the signal assigned to $P_{2/5}$ is downfield shifted following the same order, whereas the effect on the $P_{3/4}$ signal is rather small (for assignment see Fig. 1). While this trend should depend on various electronic and steric factors, it correlates well with the folding of the P_5 moiety (*vide supra*). The $^nJ_{P-P}$ ($n = 1$–2) coupling constants for all compounds are within the expected range (see ESI†). Additional $^1J_{P-B}$ coupling of 64 Hz is clearly visible in the ^{31}P NMR spectrum of **2** and is confirmed in its ^{11}B $\{^1H\}$ NMR spectrum. While the dynamic behavior of the Si-substituted compound **6** in CD_2Cl_2 solution, even at −80 °C, does not allow for determination of P–P coupling constants, its ^{29}Si(DEPT 135) NMR spectrum shows a clear doublet of

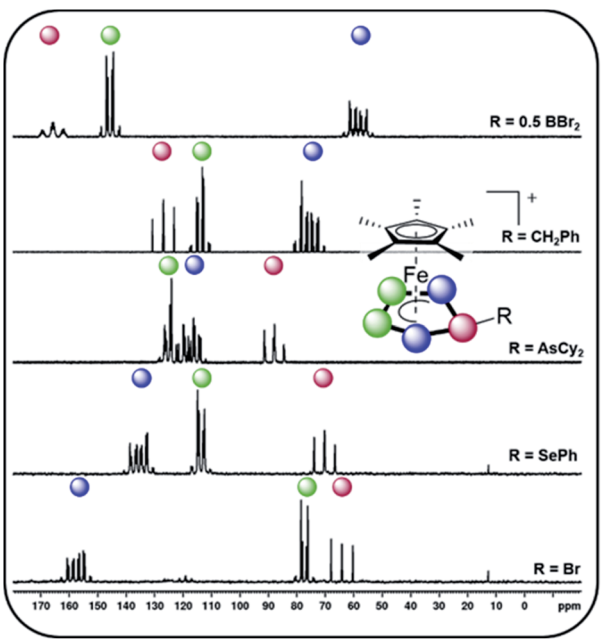

Fig. 2 $^{31}P\{^1H\}$ NMR spectra of **2**, **4**, **7**, **9** and **12** (from top to bottom, representing substitution with electrophiles from each group within the p-block) recorded in CD_2Cl_2 at room temperature and signal assignment according to the color code; respective NMR spectra of all other compounds are given in the ESI.†

multiplets at $\delta = -20$ ppm with a $^{1}J_{Si-P} = 239$ Hz coupling constant. Compared to the $SiEt_3$-substituted derivative ($^{1}J_{P-Si} = 61$ Hz), this rather large $^{1}J_{P-Si}$ coupling constant may be the result of the difference in the substitution at Si and the resulting change in the orbital contribution to the P–Si bonding interaction. Furthermore, the ^{31}P NMR spectrum of **9** reveals ^{77}Se satellites for the P_X signal and a clear doublet ($^{1}J_{P-Se} = 418$ Hz) at $\delta = 287.3$ ppm in the $^{77}Se\{^{1}H\}$ NMR spectrum.

Computational studies

To attain a better understanding of the electronic structure of the obtained complexes **2–13**, computational analyses at the B3LYP[32]/def2-TZVP[33] level of theory were performed.

Employing solvent correction,[34] the molecular structures, determined in the solid state, are well reproduced by these computations. NBO analysis[35] indicates the interaction between the $[Cp'''SbI]^+$ fragment and **1** in **8** to be of a mostly electrostatic and dispersive nature as shown by the absence of bonding MOs and the low charge transfer from the electrophile (see ESI†). Furthermore, the Wiberg Bond Indices (WBIs) for the P1–E bonds in **3** (E = Ga, WBI = 0.58/0.57) and **6** (E = Si, WBI = 0.72) suggest these bonds to be of polar single bond character. This is substantiated by the respective orbital contributions to the P1–E bonding (**3**: 79% P/21% Ga, **6**: 72% P/28% Si) and unoccupied antibonding (**3**: 21% P/79% Ga, **6**: 28% P/72% Si) molecular orbitals and agrees with the respective bond lengths determined for **3** (2.410(1)/2.387(1) Å) and **6** (2.3053(8) Å). In contrast, the WBIs of all other pentaphosphole complexes corroborate the P_1–E single bonds (WBI = 0.82–0.99) determined from their respective solid-state structures (Table 1, column 3). Accordingly, the orbital contributions to the respective P_1–E bonding and antibonding molecular orbitals (Fig. 3, left) are more balanced (Table 1, column 2), suggesting more covalent bonding in these cases. Analyzing the summed up natural charges for the fragments $\{Cp^*Fe(\eta^5\text{-}P_5)\}$ ({**1**}) and $\{R_nE\}$ ({E}, n = 1–3) (see ESI†) of **2–13** reveals correlation between the positive charge accumulation at {**1**} and the electronegativity of the central atom of the electrophiles. As **3** and **6** incorporate the least electronegative central atoms in the respective electrophile, they show the lowest charge accumulation at {**1**} in the series of the herein reported pentaphosphole complexes (see Table S13†). The charge transfer from {**1**} to {E} (Table 1, column 5) obtained by an extended charge decomposition analysis (ECDA)[36] on the optimized structures of **2–13** shows a similar trend but hints towards other factors to be of relevance as well. Thus, effective charge transfer seems to be at least one of the governing factors for the formation of covalent P_1–E bonds and consequently less labile pentaphosphole ligands, which is in line with the highly dynamic behavior of **3** and **6** in CD_2Cl_2 solution (*vide supra*). Similar to the parent compound $[Cp^*Fe(\eta^5\text{-}P_5H)]^+$,[20] the pentaphosphole complexes **2–7** and **9–13** exhibit a pronounced P_1–Fe bonding interaction (Fig. 3, right), which is represented by WBIs of 0.34–0.36. This interaction manifests their η^5-binding mode and hints towards the aromatic character of the pentaphosphole ligands. To clarify the latter point, we computed the NICS(0/1/−1)$_{zz}$[37] values for the ligand geometries from the optimized structures of the cations **2–7** and **9–13** on the PBE0 (ref. 38)/aug-pcSseg-1 (ref. 39)/def2-TZVPPD[33,40] level of theory. Consequently, these NICS(±1)$_{zz}$ values (Table 1) corroborate the aromaticity of the *cyclo*-P_5R ligands but are smaller than the ones for the *cyclo*-P_5^- ligand in

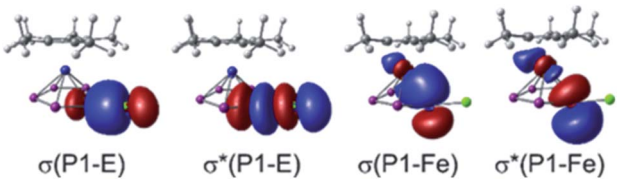

Fig. 3 Selected representative NBOs for the bonding and antibonding molecular orbitals for the P_1–E and P_1–Fe interactions found in the pentaphosphole complexes **2–7** and **9–13** exemplified at **11**; the σ* orbitals are unoccupied.

Table 1 Selected computational and experimental parameters for the pentaphosphole complexes **2–7** and **9–13**

			$d(P_1\text{–E})$/Å			
Compound	WBI (P_1–E)	Orbital contribution P_1–E	Exp.	Theo.	Charge transfer {**1**} → {E}[b]	NICS(±1)$_{zz}$[c]
2[a]	0.89	57/43	1.985(7)	2.01	0.57[d]	−31.2/−30.5
3[a]	0.58	79/21	2.399(1)	2.46	0.56[d]	−34.7/−34.3
4	0.92	45/55	1.853(4)	1.86	0.85	−33.7/−32.8
5	0.88	45/55	1.866(4)	1.89	0.84	−31.2/−32.1
6	0.72	72/28	2.3053(8)	2.35	0.68	−34.3/−34.7
7	0.82	67/33	2.348(1)	2.38	0.63	−34.0/−33.4
9	0.98	53/47	2.2234(7)	2.25	0.83	−33.5/−32.6
10	0.92	62/38	2.438(2)	2.48	0.74	−34.9/−34.0
11	0.96	36/64	—	2.03	1.09	−31.0/−30.9
12	0.98	41/59	—	2.21	1.05	−31.8/−31.7
13	0.99	51/49	2.385(1)	2.42	0.94	−34.3/−34.2

[a] As **2** and **3** are dinuclear complexes the average of the actual values is provided for clarity, NICS values have only been obtained on one the P_5 rings. [b] The charge transfer from fragment {**1**} to the respective fragments {E} is obtained by ECDA. [c] NICS(±1)$_{zz}$ values are computed on the ligand geometries from the optimized structures of the complexes **2–7** and **9–13** after removal of the $\{Cp^*Fe\}^+$ fragments. [d] The charge transfer is given per fragment {**1**}.

1 (NICS$(\pm1)_{zz}$ = −40.5). However, they compare well with that determined for the parent pentaphosphole complex [Cp*Fe(η^5-P_5H)]$^+$ (NICS$(\pm-1)_{zz}$ = −32.1/−31.2).[20] A rough correlation between the pyramidalization at P_1 and the computed NICS values is observed, although this effect is not much accentuated and has minor exceptions (see ESI†).

Thus, we demonstrated the *in situ* electrophilic functionalization of **1** to be a highly versatile approach towards a variety of unprecedented hetero-pentaphosphole complexes. Moreover, to provide a first insight into the generality of this synthetic strategy, we extended our investigations to the electrophilic functionalization of [Cp‴Ta(CO)$_2$(η^4-P_4)] (**14**)[41] bearing an aromatic tetra-phospha-*cyclo*-butadiendiide (*cyclo*-P_4^{2-}) ligand. First reactivity studies reveal that two equivalents of **14** react with BBr_3 in the presence of Tl[TEF] to afford [{Cp‴Ta(CO)$_2$}$_2${μ,$\eta^{4:4}$-((P_4)$_2$$BBr_2$)}][TEF] (**15**) in 74% yield (Fig. 4). Compound **15** crystallizes as orange blocks and shows a similar dinuclear structure as found in **2**, which was confirmed by X-ray structural analysis (Fig. 4). Interestingly, the metal fragments in **15** are rotated by nearly 180° compared to those in **2** and the P_1/P_5 atoms are bent out of the former P_4 plane by only 1.2(2)/0.7(2)°, respectively. The P–P bond lengths (2.124(4) – 2.171(4) Å) in the {(*cyclo*-P_4)$_2$$BBr_2$} ligand are slightly shortened compared to the starting material **14** (2.1555(15) – 2.1800(15) Å),[41] but still in-between covalent P–P single (2.22 Å) and double bonds (2.04 Å).[31] The P_1/P_5–B bond lengths (1.997(10)/1.996(9) Å) are within the expected range for P–B single bonds (1.96 Å) and the P_1–B–P_5 angle of 112.3(5)° leads to a slightly distorted tetrahedral geometry around the B atom. The ^{31}P NMR spectrum of **15** in CD_2Cl_2 reveals a complicated $A_2A'_2MM'XX'Z$ (Z = B) spin system with resonances located at −15.4, −37.1 and −80.8 ppm, agreeing with its structure being retained in solution. $^1J_{P-B}$ coupling is clearly visible for the $P_{M/M'}$ resonance and consequently the respective ^{11}B{^{1}H} NMR spectrum shows a triplet at −10.2 ppm with a $^1J_{P-B}$ coupling constant of 60 Hz.

The solid-state structure of **15** is well reproduced by DFT calculations (B3LYP[32]/def2-TZVP,[33] PCM solvent correction for CH_2Cl_2) which give further insight into its electronic structure. The WBIs for the P_1/P_5–B bonds (0.88/0.86) in **15** are in agreement with covalent P–B single bonds. Furthermore, the orbital contributions to these P–B bonds (58% P/42% B%) are in line with this formulation. While the positive charge within **15** is distributed across both {**14**} fragments, the B atom shows negative charge accumulation (natural charge of −0.44), labelling the {(*cyclo*-P_4)$_2$$BBr_2$} ligand in **15** a borate-bridged bis-tetraphospha-butadiendiide. At last, the respective NICS$(\pm1)_{zz}$ values indicate the aromaticity of the *cyclo*-P_4 ligand of **14** (−3.3/−3.5) to be preserved within the ligand geometry in **15** (−9.5/−9.7, −10.8/−9.6), although it is less pronounced than in the pentaphosphole complexes **2–7** and **9–13**.

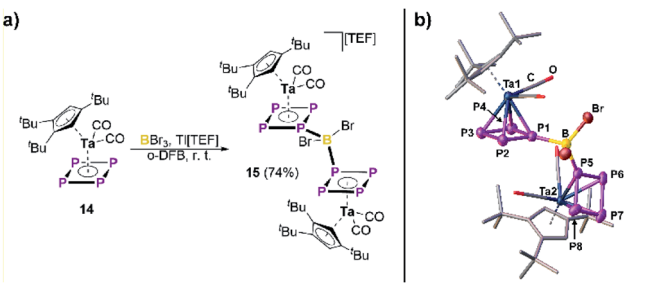

Fig. 4 (a) Reactivity of **14** towards the *in situ* formed dibromoborinium ion "[BBr_2][TEF]"; (b) molecular structure of **15** in the solid state (hydrogen atoms and the counter ion are omitted for clarity and thermal ellipsoids are drawn at the 50% probability level).

Conclusions

In conclusion, we demonstrated a general synthetic strategy to obtain a broad range of hetero-pentaphosphole coordination complexes bearing substituents from across the whole p-block of the periodic table. While the group **14–17** substituted species [Cp*Fe(η^5-P_5E)]$^+$ (E = CH_2Ph (**4**), $CHPh_2$ (**5**), $SiHPh_2$ (**6**), $AsCy_2$ (**7**), SePh (**9**), TeMes (**10**), Cl (**11**), Br (**12**), I (**13**)) reveal the desired mononuclear aromatic pentaphosphole complexes, the group 13 functionalized species result in unexpected dinuclear complexes [{Cp*Fe}$_2${μ,$\eta^{5:5}$-(P_5)$_2$$EX_2$}][TEF] ($EX_2$ = BBr_2 (**2**), GaI_2 (**3**)) with bridging bis-pentaphosphole {(*cyclo*-P_5)$_2$$EX_2$} ligands. In contrast, the alternation of the electronic and steric properties of the employed electrophile, as in [Cp‴Sb]$^+$, leads to the formation of the triple-decker-like arrangement observed in [Cp*Fe(μ,$\eta^{5:2}$-P_5)SbICp‴][TEF] (**8**). This paves the way towards the investigation of the chemical, physical and electronic properties of these all-P congeners of prototypical cyclopentadienes, which have raised considerable theoretical interest over the past decades.[8] Furthermore, this report highlights the versatility of the electrophilic functionalization of transition metal-stabilized polyphosphorus frameworks. While some P–E bond formation processes at such compounds have been observed, these are highly specific towards certain electrophile/nucleophile combinations (*vide supra*). In contrast, our approach shows an unprecedented diversity and thus allows P–E bond formation for elements all across the p-block. The generality of this approach is proven by the additional electrophilic aromatic functionalization of the aromatic *cyclo*-P_4 ligand of **14**, which furnishes [{Cp‴Ta(CO)$_2$}$_2$(μ,$\eta^{4:4}$-(P_4)$_2$$BBr_2$)][TEF] (**15**), bearing a unique borate-bridged bis-tetra-phospha-butadiendiide ligand. Finally, the obtained cationic pentaphosphole complexes **2–13** represent highly interesting starting materials (*e.g.* the halogen derivatives **11–13**) towards even further functionalized polyphosphorus frameworks, which is underlined by the gram scale synthesis of selected representatives (**5**, **11–13**).

Data availability

Crystallographic data for **2–10**, **13** and **15** has been deposited at the CCDC/ICSD under 2083554 (**2**), 2083555 (**3**), 2083556 (**4**), 2083557 (**5**), 2083558 (**6**), 2083559 (**7**), 2083560 (**8**), 2083561 (**9**), 2083562 (**10**), 2083563 (**13**) and 2101248 (**15**). All other data are provided in this article or in the ESI.†

Author contributions

C. R. performed the experimental work and wrote the original draft. G. B. assisted in the performance of DFT calculations. M. Seidl assisted in the interpretation of X-ray structural data and M. Scheer supervised and acquired funding for the project. All authors contributed in preparing the final manuscript.

Conflicts of interest

There are no conflicts to declare.

Acknowledgements

This work was supported by the Deutsche Forschungsgemeinschaft (DFG, Sche 384/36-1). C. R. is grateful to the Studienstiftung des Deutschen Volkes for his PhD fellowship. This paper is dedicated to Professor Werner Thiel on the occasion of his 60th birthday.

References

1 (*a*) C. Friedel and J. M. Crafts, *Compt. Rend.*, 1877, **84**, 1392; (*b*) C. Friedel and J. M. Crafts, *Compt. Rend.*, 1877, **84**, 1450.
2 (*a*) R. Brückner, *Reaktionsmechanismen*, Springer, Berlin, Heidelberg, 2004, pp. 203–235; (*b*) P. Y. Bruice, *Organische Chemie*, Pearson Studium, Hallbergmoos, 2013, pp. 627–642.
3 (*a*) T. J. Kealy and P. L. Pauson, *Nature*, 1951, **168**, 1039–1040; (*b*) R. B. Woodward, M. Rosenblum and M. C. Whiting, *J. Am. Chem. Soc.*, 1952, **74**, 3458–3459.
4 E. O. Fischer and K. Öfele, *Chem. Ber.*, 1957, **90**, 2532–2535.
5 R. Hoffmann, *Angew. Chem., Int. Ed. Engl.*, 1982, **21**, 711–724.
6 (*a*) M. Baudler and T. Etzbach, *Chem. Ber.*, 1991, **124**, 1159–1160; (*b*) V. A. Milyukov, A. V. Kataev, O. G. Sinyashin and E. Hey-Hawkins, *Russ. Chem. Bull.*, 2006, **55**, 1297–1299; (*c*) M. Jo, A. Dragulescu-Andrasi, L. Z. Miller, C. Pak and M. Shatruk, *Inorg. Chem.*, 2020, **59**, 5483–5489.
7 M. Baudler, S. Akpapoglou, D. Ouzounis, F. Wasgestian, B. Meinigke, H. Budzikiewicz and H. Münster, *Angew. Chem., Int. Ed. Engl.*, 1988, **27**, 280–281.
8 (*a*) L. Nyulászi, *Inorg. Chem.*, 1996, **35**, 4690–4693; (*b*) M. N. Glukhovtsev, A. Dransfeld and P. v. R. Schleyer, *J. Phys. Chem.*, 1996, **100**, 13447–13454; (*c*) A. Dransfeld, L. Nyulászi and P. v. R. Schleyer, *Inorg. Chem.*, 1998, **37**, 4413–4420; (*d*) M. K. Cyrański, P. v. R. Schleyer, T. M. Krygowski, H. Jiao and G. Hohlneicher, *Tetrahedron*, 2003, **59**, 1657–1665; (*e*) W. P. Ozimiński and J. C. Dobrowolski, *Chem. Phys.*, 2005, **313**, 123–132; (*f*) L. Wang, H. J. Wang, W. B. Dong, Q. Y. Ge and L. Lin, *Struct. Chem.*, 2007, **18**, 25–31; (*g*) W.-Q. Li, L.-L. Liu, J.-K. Feng, Z.-Z. Liu, A.-M. Ren, G. Zhang and C.-C. Sun, *J. Theor. Comput. Chem.*, 2008, **07**, 1203–1214; (*h*) D. Josa, A. Peña-Gallego, J. Rodríguez-Otero and E. M. Cabaleiro-Lago, *J. Mol. Model.*, 2011, **17**, 1267–1272.
9 (*a*) O. J. Scherer and T. Brück, *Angew. Chem., Int. Ed. Engl.*, 1987, **26**, 59; (*b*) M. Baudler and T. Etzbach, *Angew. Chem., Int. Ed. Engl.*, 1991, **30**, 580–582; (*c*) A. R. Kudinov, D. A. Loginov, Z. A. Starikova, P. V. Petrovskii, M. Corsini and P. Zanello, *Eur. J. Inorg. Chem.*, 2002, **2002**, 3018–3027; (*d*) E. Urnius, W. W. Brennessel, C. J. Cramer, J. E. Ellis and P. v. R. Schleyer, *Science*, 2002, **295**, 832–834; (*e*) C. M. Knapp, B. H. Westcott, M. A. C. Raybould, J. E. McGrady and J. M. Goicoechea, *Angew. Chem., Int. Ed.*, 2012, **51**, 9097–9100; (*f*) S. Heinl, G. Balázs, M. Bodensteiner and M. Scheer, *Dalton Trans.*, 2016, **45**, 1962–1966.
10 (*a*) B. M. Cossairt, N. A. Piro and C. C. Cummins, *Chem. Rev.*, 2010, **110**, 4164–4177; (*b*) M. Caporali, L. Gonsalvi, A. Rossin and M. Peruzzini, *Chem. Rev.*, 2010, **110**, 4178–4235; (*c*) C. M. Hoidn, D. J. Scott and R. Wolf, *Chem.– Eur. J.*, 2021, **27**, 1886–1902.
11 (*a*) J. Bai, A. V. Virovets and M. Scheer, *Angew. Chem., Int. Ed.*, 2002, **41**, 1737–1740; (*b*) J. Bai, A. V. Virovets and M. Scheer, *Science*, 2003, **300**, 781–783; (*c*) M. Scheer, J. Bai, B. P. Johnson, R. Merkle, A. V. Virovets and C. E. Anson, *Eur. J. Inorg. Chem.*, 2005, **2005**, 4023–4026; (*d*) M. Scheer, L. J. Gregoriades, A. V. Virovets, W. Kunz, R. Neueder and I. Krossing, *Angew. Chem., Int. Ed.*, 2006, **45**, 5689–5693; (*e*) M. Scheer, A. Schindler, R. Merkle, B. P. Johnson, M. Linseis, R. Winter, C. E. Anson and A. V. Virovets, *J. Am. Chem. Soc.*, 2007, **129**, 13386–13387; (*f*) S. Welsch, L. J. Gregoriades, M. Sierka, M. Zabel, A. V. Virovets and M. Scheer, *Angew. Chem., Int. Ed.*, 2007, **46**, 9323–9326; (*g*) M. Scheer, L. J. Gregoriades, R. Merkle, B. P. Johnson and F. Dielmann, *Phosphorus, Sulfur Silicon Relat. Elem.*, 2008, **183**, 504–508; (*h*) M. Scheer, A. Schindler, C. Gröger, A. V. Virovets and E. V. Peresypkina, *Angew. Chem., Int. Ed.*, 2009, **48**, 5046–5049; (*i*) M. Scheer, A. Schindler, J. Bai, B. P. Johnson, R. Merkle, R. Winter, A. V. Virovets, E. V. Peresypkina, V. A. Blatov, M. Sierka and H. Eckert, *Chem.– Eur. J.*, 2010, **16**, 2092–2107; (*j*) F. Dielmann, A. Schindler, S. Scheuermayer, J. Bai, R. Merkle, M. Zabel, A. V. Virovets, E. V. Peresypkina, G. Brunklaus, H. Eckert and M. Scheer, *Chem.– Eur. J.*, 2012, **18**, 1168–1179; (*k*) E. Peresypkina, C. Heindl, A. Virovets, H. Brake, E. Mädl and M. Scheer, *Chem.– Eur. J.*, 2018, **24**, 2503–2508.
12 M. V. Butovskiy, G. Balázs, M. Bodensteiner, E. V. Peresypkina, A. V. Virovets, J. Sutter and M. Scheer, *Angew. Chem., Int. Ed.*, 2013, **52**, 2972–2976.
13 E. Mädl, M. V. Butovskii, G. Balázs, E. V. Peresypkina, A. V. Virovets, M. Seidl and M. Scheer, *Angew. Chem., Int. Ed.*, 2014, **53**, 7643–7646.
14 (*a*) F. Riedlberger, S. Todisco, P. Mastrorilli, A. Y. Timoshkin, M. Seidl and M. Scheer, *Chem.– Eur. J.*, 2020, **26**, 16251–16255; (*b*) R. Yadav, T. Simler, S. Reichl, B. Goswami, C. Schoo, R. Köppe, M. Scheer and P. W. Roesky, *J. Am. Chem. Soc.*, 2020, **142**, 1190–1195.
15 D. Tofan, B. M. Cossairt and C. C. Cummins, *Inorg. Chem.*, 2011, **50**, 12349–12358.
16 (*a*) J. J. Weigand, M. Holthausen and R. Fröhlich, *Angew. Chem., Int. Ed.*, 2009, **48**, 295–298; (*b*) M. H. Holthausen and J. J. Weigand, *Chem. Soc. Rev.*, 2014, **43**, 6639–6657.

17 A. K. Adhikari, C. G. P. Ziegler, K. Schwedtmann, C. Taube, J. J. Weigand and R. Wolf, *Angew. Chem., Int. Ed.*, 2019, **58**, 18584–18590.
18 C. G. P. Ziegler, T. M. Maier, S. Pelties, C. Taube, F. Hennersdorf, A. W. Ehlers, J. J. Weigand and R. Wolf, *Chem. Sci.*, 2019, **10**, 1302–1308.
19 R. Yadav, B. Goswami, T. Simler, C. Schoo, S. Reichl, M. Scheer and P. W. Roesky, *Chem. Commun.*, 2020, **56**, 10207–10210.
20 C. Riesinger, G. Balázs, M. Bodensteiner and M. Scheer, *Angew. Chem., Int. Ed.*, 2020, **59**, 23879–23884.
21 S. J. Connelly, W. Kaminsky and D. M. Heinekey, *Organometallics*, 2013, **32**, 7478–7481.
22 (*a*) A. Jayaraman, T. V. Jacob, J. Bisskey and B. T. Sterenberg, *Dalton Trans.*, 2015, **44**, 8788–8791; (*b*) A. Jayaraman and B. T. Sterenberg, *Organometallics*, 2016, **35**(14), 2367–2377; (*c*) A. Jayaraman, S. Nilewar, T. V. Jacob and B. T. Sterenberg, *ACS Omega*, 2017, **2**, 7849–7861.
23 (*a*) G. Capozzi, L. Chiti, M. Di Vaira, M. Peruzzini and P. Stoppioni, *Chem. Commun.*, 1986, **24**, 1799–1800; (*b*) A. Barth, G. Huttner, M. Fritz and L. Zsolnai, *Angew. Chem., Int. Ed. Engl.*, 1990, **29**, 929–931; (*c*) P. Barbaro, A. Ienco, C. Mealli, M. Peruzzini, O. J. Scherer, G. Schmitt, F. Vizza and G. Wolmershäuser, *Chem.– Eur. J.*, 2003, **9**, 5196–5210; (*d*) M. Peruzzini, R. R. Abdreimova, Y. Budnikova, A. Romerosa, O. J. Scherer and H. Sitzmann, *J. Organomet. Chem.*, 2004, **689**, 4319–4331; (*e*) B. M. Cossairt, M.-C. Diawara and C. C. Cummins, *Science*, 2009, **323**, 602; (*f*) P. Barbaro, C. Bazzicalupi, M. Peruzzini, S. Seniori Costantini and P. Stoppioni, *Angew. Chem., Int. Ed.*, 2012, **51**, 8628–8631; (*g*) C. Schwarzmaier, S. Heinl, G. Balázs and M. Scheer, *Angew. Chem., Int. Ed.*, 2015, **54**, 13116–13121; (*h*) E. Mädl, G. Balázs, E. V. Peresypkina and M. Scheer, *Angew. Chem., Int. Ed.*, 2016, **55**, 7702–7707; (*i*) A. Cavaillé, N. Saffon-Merceron, N. Nebra, M. Fustier-Boutignon and N. Mézailles, *Angew. Chem., Int. Ed.*, 2018, **57**, 1874–1878; (*j*) C. M. Hoidn, T. M. Maier, K. Trabitsch, J. J. Weigand and R. Wolf, *Angew. Chem., Int. Ed.*, 2019, **58**, 18931–18936; (*k*) U. Chakraborty, J. Leitl, B. Mühldorf, M. Bodensteiner, S. Pelties and R. Wolf, *Dalton Trans.*, 2018, **47**, 3693–3697.
24 (*a*) C. Dohmeier, C. Robl, M. Tacke and H. Schnöckel, *Angew. Chem., Int. Ed. Engl.*, 1991, **30**, 564–565; (*b*) S. Schulz, H. W. Roesky, H. J. Koch, G. M. Sheldrick, D. Stalke and A. Kuhn, *Angew. Chem., Int. Ed. Engl.*, 1993, **32**, 1729–1731; (*c*) R. Yadav, T. Simler, B. Goswami, C. Schoo, R. Köppe, S. Dey and P. W. Roesky, *Angew. Chem., Int. Ed.*, 2020, **59**, 9443–9447.
25 A. Frei, *Chem.– Eur. J.*, 2019, **25**, 7074–7090.
26 (*a*) I. Krossing, *Chem.– Eur. J.*, 2001, **7**, 490–502; (*b*) M. Gonsior, I. Krossing and N. Mitzel, *Z. Anorg. Allg. Chem.*, 2002, **628**, 1821.
27 (*a*) N. Burford, P. J. Ragogna, R. McDonald and M. J. Ferguson, *J. Am. Chem. Soc.*, 2003, **125**, 14404–14410; (*b*) M. Gonsior, I. Krossing, L. Müller, I. Raabe, M. Jansen and L. van Wüllen, *Chem.– Eur. J.*, 2002, **8**, 4475–4492; (*c*) J. Possart, A. Martens, M. Schleep, A. Ripp, H. Scherer, D. Kratzert and I. Krossing, *Chem.– Eur. J.*, 2017, **23**, 12305–12313.
28 G. Manca and A. Ienco, *Inorg. Chim. Acta*, 2021, **517**, 120205.
29 H. Brake, E. Peresypkina, A. V. Virovets, M. Piesch, W. Kremer, L. Zimmermann, C. Klimas and M. Scheer, *Angew. Chem., Int. Ed.*, 2020, **59**, 16241–16246.
30 A. Garbagnati, M. Seidl, G. Balázs and M. Scheer, *Inorg. Chem.*, 2021, **60**, 5163–5171.
31 (*a*) P. Pyykkö and M. Atsumi, *Chem.– Eur. J.*, 2009, **15**, 186–197; (*b*) P. Pyykkö and M. Atsumi, *Chem.– Eur. J.*, 2009, **15**, 12770–12779; (*c*) P. Pyykkö, *J. Phys. Chem. A*, 2015, **119**, 2326–2337.
32 (*a*) P. A. M. Dirac, *Proc. R. Soc. London, Ser. A*, 1929, **123**, 714–733; (*b*) J. C. Slater, *Phys. Rev.*, 1951, **81**, 385–390; (*c*) S. H. Vosko, L. Wilk and M. Nusair, *Can. J. Phys.*, 1980, **58**, 1200–1211; (*d*) C. Lee, W. Yang and R. G. Parr, *Phys. Rev. B: Condens. Matter Mater. Phys.*, 1988, **37**, 785–789; (*e*) A. D. Becke, *Phys. Rev. A*, 1988, **38**, 3098–3100; (*f*) A. D. Becke, *J. Chem. Phys.*, 1993, **98**, 5648–5652.
33 (*a*) F. Weigend and R. Ahlrichs, *Phys. Chem. Chem. Phys.*, 2005, **7**, 3297–3305; (*b*) F. Weigend, *Phys. Chem. Chem. Phys.*, 2006, **8**, 1057–1065.
34 J. Tomasi, B. Mennucci and R. Cammi, *Chem. Rev.*, 2005, **105**, 2999–3093.
35 (*a*) E. D. Glendening, C. R. Landis and F. Weinhold, *J. Comput. Chem.*, 2013, **34**, 1429–1437; (*b*) E. D. Glendening, C. R. Landis and F. Weinhold, *J. Comput. Chem.*, 2013, **34**, 2134.
36 (*a*) S. Dapprich and G. Frenking, *J. Phys. Chem.*, 1995, **99**, 9352–9362; (*b*) M. Xiao and T. Lu, *J. Adv. Phys. Chem.*, 2015, **04**, 111–124.
37 (*a*) P. v. R. Schleyer, C. Maerker, A. Dransfeld, H. Jiao and N. J. R. van Eikema Hommes, *J. Am. Chem. Soc.*, 1996, **118**, 6317–6318; (*b*) Z. Chen, C. S. Wannere, C. Corminboeuf, R. Puchta and P. v. R. Schleyer, *Chem. Rev.*, 2005, **105**, 3842–3888; (*c*) T. Lu and F. Chen, *J. Comput. Chem.*, 2012, **33**, 580–592.
38 (*a*) J. P. Perdew, K. Burke and M. Ernzerhof, *Phys. Rev. Lett.*, 1996, **77**, 3865–3868; (*b*) J. P. Perdew, K. Burke and M. Ernzerhof, *Phys. Rev. Lett.*, 1997, **78**, 1396; (*c*) C. Adamo and V. Barone, *J. Chem. Phys.*, 1999, **110**, 6158–6170.
39 F. Jensen, *J. Chem. Theory Comput.*, 2015, **11**, 132–138.
40 (*a*) B. Metz, H. Stoll and M. Dolg, *J. Chem. Phys.*, 2000, **113**, 2563–2569; (*b*) K. A. Peterson, D. Figgen, E. Goll, H. Stoll and M. Dolg, *J. Chem. Phys.*, 2003, **119**, 11113–11123; (*c*) D. Rappoport and F. Furche, *J. Chem. Phys.*, 2010, **133**, 134105.
41 F. Dielmann, E. V. Peresypkina, B. Krämer, F. Hastreiter, B. P. Johnson, M. Zabel, C. Heindl and M. Scheer, *Angew. Chem., Int. Ed.*, 2016, **55**, 14833–14837.